ONLINE FIRST

This is a provisional PDF only. Copyedited and fully formatted version will be made available soon.

REPORTS OF PRACTICAL ONCOLOGY AND RADIOTHERAPY

ISSN: 1507-1367

e-ISSN: 2083-4640

Impact of MLC error on dose distribution in SRS treatment of single-isocenter multiple brain metastases: Comparison between DCAT and VMAT techniques

Authors: Hiroki Katayama, Takuya Kobata, Motonori Kitaoka, Shigeo Takamashi, Toru Shibata

DOI: 10.5603/rpor.102616

Article type: Research paper

Published online: 2024-09-27

Impact of MLC error on dose distribution in SRS treatment of single-isocenter multiple brain metastases: Comparison between DCAT and VMAT techniques

Running Head: Impact of MLC error on dose of DCAT and VMAT

DOI: 10.5603/rpor.102616

Hiroki Katayama[1], Takuya Kobata[1], Motonori Kitaoka[1], Shigeo Takahashi[2], and Toru Shibata[2]

[1]*Department of Clinical Radiology, Kagawa University Hospital, Kagawa, Japan*

[2]*Department of Radiation Oncology, Kagawa University Hospital, Kagawa, Japan*

Corresponding author: Hiroki Katayama, Ph.D., Department of Clinical Radiology, Kagawa University Hospital, Kagawa, Japan 1750-1 Ikenobe, Miki-cho, Kita-gun, Kagawa 761-0793, Japan, tel: (+81)87-898-5111, fax: (+81)87-891-2351; e-mail: katayama.hiroki@kagawa-u.ac.jp

Abstract

Background: Dynamic conformal arc therapy (DCAT) and volumetric modulated arc therapy (VMAT) can achieve near equal plan quality in single-isocenter multiple target stereotactic radiosurgery (SRS) for brain metastases. This study aimed to investigate the impact of multi-leaf collimator (MLC) errors during beam delivery on the dose distribution for each technique.

Materials and methods: A 10-mm diameter delineation of the three targets was employed on the computed tomography images of a head phantom, and the reference plans were created using the DCAT and VMAT. We simulated the systematic opened and closed MLC errors. 10 MLC error plans with different magnitudes of errors were created in each technique. We investigated the relationship between the magnitude of MLC errors and the change in dose-volume histogram parameters of the targets and normal brain tissue.

Results: The percentage change in the $D_{98\%}$ (Gy) and $D_{0.1\%}$ (Gy) of the target per millimeter of the MLC errors were 13.3% and 2.7% for the DCAT and 15.3% and 9.3% for the VMAT, respectively. The fluctuations of the maximum dose were very small for the DCAT compared to the VMAT. Changes in the V_{12Gy} (cc) of the normal brain tissue were 47.1%/mm and 53.2%/mm for the DCAT and VMAT, respectively, which are comparable changes for both techniques.

Conclusions: Although the impact of MLC errors on the target coverage and the normal brain tissue is comparable for both techniques, the internal dose of the targets generated by the DCAT technique is robust to the MLC errors.

Key words: brain SRS; DCAT; VMAT; MLC error; single-isocenter

Introduction

Single-isocenter multiple target stereotactic radiosurgery (SRS) for brain metastases based on the linear accelerator can be performed using the treatment techniques of dynamic conformal arc therapy (DCAT) or volumetric modulated arc therapy (VMAT) [1–5]. Both irradiation techniques can create a high-dose and steep dose distribution to the target using a multi-leaf collimator (MLC).

The VMAT technique requires a strict MLC position accuracy because they move dramatically during beam delivery. Oliver et al. [6] reported that the systematic MLC errors should be < 0.6 mm for the head and neck VMAT. Deng et al. [7] reported that the systematic MLC opening error and closing error should be less than 0.32 mm and 0.38 mm, respectively, in the stereotactic body radiotherapy (SBRT)-VMAT for non-small cell lung cancer,. Thus, for smaller target regions, such as a brain metastasis, a more stringent MLC position accuracy will be required for the VMAT. Conversely, the MLC segments of the DACT technique are always opened during beam delivery, and the MLC was fitted to the edges of the target. However, the dose distribution may be strongly affected by the MLC position errors because the target volume is significantly small. In previous studies, several researchers have focused on the attainable plan quality with the treatment planning system (TPS) for the single-isocenter multiple target SRS treatment, comparing the DCAT and

VMAT techniques. Ruggieri et al. [8] reported that both techniques can achieve the near equal plan quality.

However, the impact of the MLC errors on the dose distributions may be different, even if the same dose distribution could be produced by both techniques. These differences need to be clarified to ensure quality control (QC) of the MLC position and the commissioning of TPS in each treatment technique.

We evaluated the change in the dose distribution on the targets and organ at risk (OAR) by simulating the MLC errors for the DCAT and VMAT techniques using the TPS and anthropomorphic head phantom. First, we created a reference plan and systematic opened and closed MLC error plans and investigated the relationship between the magnitude of MLC errors and change in dose-volume histogram (DVH) parameters for the two techniques. Next, gamma analysis was performed on the MLC error plans to evaluate the agreement with the dose distribution of the reference plan.

Materials and methods

Phantom objects and computed tomography (CT) acquisition

A STEEV phantom (CIRS, Norfolk, VA, USA) was used. CT images were acquired using an Aquilion LB (Canon Medical Systems Corp., Tokyo, Japan), with a 1-mm slice thickness.

Treatment planning

DCAT with reference plan

A 10-mm diameter delineation of the three targets was employed on the CT images, which were defined as gross tumor volumes (GTVs). First, the DCAT plan was constructed using the Elements Multiple Brain Mets SRS ver.3.0 (Elements MBM, Brainlab, Munich, Germany). The GTVs were expanded by 1 mm in all directions to form the planning target volumes (PTVs), which were defined as PTV_a, PTV_b and PTV_c. Figure 1A shows the targets position on the CT images. The distance between isocenter and each PTV was approximately 2 cm. The treatment plan was created using TrueBeam linear accelerator 6 MV FFF photons (Varian Medical Systems, Palo Alto, CA, USA) with

Millennium 120-MLC (5 mm width leaves). The dose of the 20 Gy per 1 fraction was prescribed to cover 98% of PTV at 80% isodose line (IDL). The max dose objective of the PTV was $D_{5\%} < 25$ Gy. Dose calculation was performed using the Monte Carlo algorithm, and the grid size was 1 mm. We performed a series of experiments with 5 mm and 15 mm as the target diameters.

We exported the DCAT plan to the Eclipse ver.16.1 (Varian Medical Systems, Palo Alto, CA). The DCAT plan was recalculated on a 1-mm grid size and 2.0° gantry steps using the AcurosXB algorithm, which was defined as the DCAT reference plan ($DCAT_{ref}$). Figure 1B shows the dose distribution of $DCAT_{ref}$ on the CT images.

VMAT with reference plan

Next, the $DCAT_{ref}$ was replanned using the VMAT technique on the Eclipse. Here, no changes were employed for the gantry angle, number of arcs, couch positions, isocenter position, collimator angle, prescribed dose, and photon energy. The dose of 20 Gy was prescribed to each PTV. Dose calculation was performed using the AcurosXB algorithm with a 1-mm grid size and 2.0° gantry steps. Finally, the plan was normalized to at least 98% of the PTV_b receiving 100% of the prescribed dose, which was defined as the VMAT reference plan ($VMAT_{ref}$).

Moreover, we calculated the Paddick conformity index (CI) [9] and gradient index (GI) [10] as indicator of the dose conformity and the dose fall-off as follows:

$$CI = \frac{(TVPTV)^2}{TV \times PIV} \qquad (1)$$

where the TVPTV is PTV volume covered by 100% of prescription dose and TV is target volume, PIV is the total volume covered by the prescribed dose.

$$GI = \frac{PIV_{half}}{PIV} \qquad (2)$$

where the PTV_{half} is the volume covered by half the prescription dose.

Table 1 shows the DVH and plan parameters of the reference plan with the DCAT and VMAT techniques. The reference plans of both techniques had nearly equivalent DVH parameters.

MLC error plan creation

The systematic opened and closed MLC position errors were simulated as these will strongly affect the dose distribution than the random MLC errors [6, 11]. We exported the DICOM-RT Plan files of the $DCAT_{ref}$ and $VMAT_{ref}$ to Python (ver. 3.8.5) from the Eclipse and changed the MLC positions using an in-house code.

The magnitudes of the simulated systematic MLC errors were ±0.1, ±0.2, ±0.3, ±0.5, and ±1.0 mm, respectively, which were added to the MLC position of reference plans in every control point for each MLC bank. Namely, the changes in the MLC gap widths of the reference plan were ±0.2, ±0.4, ±0.6, ±1.0, and ±2.0 mm. Consequently, ten MLC error plans which had different magnitudes of errors were created in each technique. The positive and the negative value indicated the opened and closed MLC errors, respectively.

However, the MLC errors were not added to the reference MLC position in the following cases: (1) If the MLC gap width is 0 at the reference plan (i.e., when the MLC positions of A and B bank were the same value) and (2) if the MLC gap width is < 0 when the closed MLC errors were added to the reference position. (This is because the MLC bank of A and B will collide). Figure 2 provides an example of the MLC position of the reference plans and MLC error plans for the DCAT and VMAT techniques.

We inserted the 10 MLC error plans back into the Eclipse and then recalculated the dose distribution under the same MU and MLC motion of the reference plans.

Plan comparison between the reference plan and MLC error plans

We calculated the difference in the DVH parameters between the reference plan and MLC error plans. The difference in $D_{98\%}$ (Gy) and $D_{0.1\%}$ (Gy) of the PTVs from the reference plan dose was calculated as follows:

$$Dose\,difference(\%) = \frac{D_{error} - D_{ref}}{D_{ref}} \times 100 \qquad (3)$$

where the D_{error} and D_{ref} are the doses for the MLC error plan and reference plan, respectively.

The difference in V_{12Gy} (cc) of the brain-PTVs from the reference plan volume was calculated as follows:

$$Volume\,difference(\%) = \frac{V_{error} - V_{ref}}{V_{ref}} \times 100 \qquad (4)$$

where the V_{error} and V_{ref} are the volumes for the MLC error plan and reference plan, respectively. We applied the linear regression analysis between the magnitude of MLC errors and the change in the DVH parameters to assess the sensitivity of the $DCAT_{ref}$ and $VMAT_{ref}$ to the MLC errors. The dose or volume percentage change per 1.0 mm of the MLC errors can be expressed as the slope value of the linear regression equation, which would be higher for the irradiation techniques that are more susceptible to MLC errors. The linear regression analysis was performed using the Microsoft Excel 2021.

Moreover, we calculated the change in CI and GI relative to the reference plan due to the MLC error as follows:

$$CI_{diff} = \frac{CI_{error} - CI_{ref}}{CI_{ref}} \times 100(\%) \qquad (5)$$

where the CI_{error} and CI_{ref} are the values of CI for the MLC error plan and reference plan, respectively.

$$GI_{diff} = \frac{GI_{error} - GI_{ref}}{GI_{ref}} \times 100(\%) \qquad (6)$$

where the GI_{error} and GI_{ref} are the values of GI for the MLC error plan and reference plan, respectively.

Gamma analysis of dose distribution between the reference plan and MLC error plans

The MIM maestro ver. 7.1 (MIM Software Inc, Cleveland, OH, USA) was used for the absolute gamma analysis between the reference plan and each MLC error plan to evaluate dose distribution changes. Local dose normalization with 2%/1 mm criteria was applied to each analysis with 10% and

40% dose threshold. We applied a threshold value of 40% to the gamma pass rate (GPR) calculation to evaluate the high-dose region (>12 Gy).

Results

Table 2 shows the slope value of the linear regression equation between the magnitude of MLC errors and change in the DVH parameters for each target diameter. R-squared values indicate >0.9 for each DVH parameter, showing high linear relationships. The slope values increased with the decreasing target diameter.

Figure 3 shows the relationship between the magnitude of MLC errors and the mean percentage difference in $D_{98\%}$ (Gy) from the reference plan for the PTVs in each target diameter. The dose percentage change in $D_{98\%}$ (Gy) due to the MLC error of −0.5 mm to + 0.5 mm had the same tendency for the two techniques, exhibiting linear correlations with the magnitude of the MLC error. Thus, the impact of MLC errors on target coverage was comparable for both techniques. For the 1.0-mm opened MLC error with the DCAT, the change in the $D_{98\%}$ (Gy) is lower than that of VMAT. This is attributed to the fact that the MLC edge is completely distant from the target border through the addition of an opened error. For the target diameter of 5 mm with the VMAT, the $D_{98\%}$ (Gy) did not linearly decrease at a closed error of 1.0 mm. This is because several MLC segments smaller than 1.0 mm were created, which hampered the addition of 1.0-mm closed errors to the reference position of the MLC.

Figure 4 shows the relationship between the magnitude of MLC errors and the mean percentage difference in $D_{0.1\%}$ (Gy) from the reference plan for the PTVs in each target diameter. Although the change in $D_{0.1\%}$ (Gy) also exhibited linear correlations with the magnitude of MLC error for both techniques, the slope values of DCAT were less than half of those of VMAT in each target diameter. Thus, the fluctuations in the maximum dose of targets with the DCAT technique were very small compared to that of the VMAT technique. The dose profiles of reference and closed MLC error plan are shown in Figure 5.

Figure 6 shows the relationship between the magnitude of MLC errors and the mean percentage difference in V_{12Gy} (cc) from the reference plan for the normal brain tissue in each target diameter. The volume percentage change in V_{12Gy} (cc) with the DCAT also closely resembled that of VMAT, the changes being comparable for both techniques in each target diameter.

Figure 7 shows the relationship between the magnitude of MLC errors and the percentage difference in CI and GI from the reference plan. The CI and GI were decreased when the opened MLC errors were added to the reference position, the changes being equivalent for the two techniques. For target diameter of 5 mm, the CI and GI were stronger changed by the MLC error.

Figure 8 shows the relationship between the magnitude of MLC errors and the GPR for each target diameter. The GPR decreased with the increase in MLC errors for both techniques, which were more pronounced for the smaller target diameter. The GPR with the DCAT technique is higher than that of the VMAT technique in each MLC error plan, except for the target diameters of 5 mm with threshold 40%. Moreover, the difference in GPR between the DCAT and VMAT was larger at the threshold value of 40% than that of 10%. These results indicated that the change in high dose regions was small for the DCAT technique.

Discussion

To the best of our knowledge, this is the first study to compare the plan robustness of the DCAT and VMAT techniques on the MLC errors in the brain SRS. Using the TPS, the impact of the MLC error on the dose distribution for the DCAT and VMAT techniques was estimated. Although the MLC errors on the target coverage, normal brain tissue, dose conformity and dose fall-off showed equivalent changes for both techniques, the maximum dose of targets generated by the DCAT technique was robust to the MLC errors compared with the VAMT technique.

The VMAT dose distribution is formed by many MLC segments (MLC gap width) smaller than the target size during beam delivery. The MLC gap width errors cause the dose errors, and the smaller the gap width, the larger the dose error [12]. Moreover, Oliver et al. [6] reported that the gap width

errors are linearly correlated with the dose deviation. Prentou et al. [13] investigated the impact of MLC error on the dose distribution for the brain SRS using the VMAT technique. They concluded that the MLC gap width error of 0.19 mm may not be clinically acceptable for the target located in close proximity to the OAR.

For DCAT techniques, MLC segment size is almost the same as that of each target size, and the MLC positions are always placed on the edge of the targets. The errors mainly related to the target border will only affect the peripheral dose of the targets. Thus, we also investigated the change in V_{12Gy} (cc) of normal brain tissue because of the predictor for radiation necrosis [14]. The dose of normal brain tissue was linearly increased by the opened MLC errors, the target conformity decreased in both irradiation techniques. Hence, our results indicated that the dose or volume changes in $D_{98\%}$ (Gy) and V_{12Gy} (cc) due to the MLC error for the DCAT were comparable to that of VMAT.

The change in the maximum dose of the target due to the MLC errors was found to be small in the DCAT technique. These results indicate the preservation of internal dose distribution of targets. This is because the MLC does not pass over the target center. Therefore, the GPR with the DCAT technique between the reference plan and the MLC error plan is higher than that of the VMAT technique. In general, the dose for brain metastases is prescribed by the IDL [15, 16]. The dose inside targets is higher than the prescription dose and is associated with the local control [17, 18]. Hence, to ensure the internal dose distribution of targets, the DCAT technique is robust when employed to the MLC errors.

Previous studies elucidated on the attainable plan quality and compared them between the DCAT and VMAT techniques [3, 19, 20]. Hofmaier et al. [21] reported that the DCAT technique performs better than the VMAT technique when the target shape is nearly spherical, while the VMAT technique is superior for irregular shapes. Torizuka et al. [20] compared the plan quality between the coplanar VMAT, non-coplanar VMAT, and DCAT technique and reported that the non-coplanar VMAT can improve the target conformity and normal brain tissue. However, the impact of MLC

errors during beam delivery on the dose distribution has never been clarified. Our results showed that the impact of MLC errors on the target coverage and normal brain tissue is comparable for both techniques. These results indicate that the QC of the MLC position for the DCAT technique would require performance at the same tolerance level as for the VMAT technique.

Moreover, the study results present the important findings for the MLC commissioning of the brain SRS. The dose error between the calculation and delivery is affected not only by the accuracy of the mechanical MLC position but also by the MLC parameters on the TPS such as the dosimetric leaf gap (DLG) and MLC transmission factor [22]. Particularly, the DLG parameter is a value that registers the rounded leaf-end transmission dose as the MLC gap width in the TPS, the tuning errors correspond to the “systematic opened or closed MLC errors”. Therefore, the DLG parameter should be adjusted during the commissioning process at each institution [23–25]. The MLC commissioning of the DCAT technique should be focused on the peripheral dose of targets because the internal dose of targets will have minimal changes as a result of DLG parameter tuning. Vieillevigne et al. [26] evaluated the impact of the DLG parameter on the dose distribution for the DCAT and VMAT techniques in the lung SBRT and brain SRS using the GPR with the 2D array detector. They reported that the DCAT exhibited an excellent agreement using the DLG value obtained from the standard sweeping gap test. However, as we have shown in the Results section, the DCAT technique had a high GPR because the measurement points dose inside the targets are consistent with the planned dose. Moreover, the GPR depends on the detector resolutions and the setting criteria [27, 28]. Thus, the loss of target coverage cannot be detected by the GPR evaluation. We revealed that the target coverage is strongly affected by the MLC errors for the DCAT technique.

This study has some limitations. First, we simulated the MLC errors using 5 mm width MLC leaves. The impact of MLC errors on smaller targets may be reduced when using the high-definition MLC (2.5 mm width leaves). However, we believe that the characteristic of DVH parameter changes due to the MLC error is identical regardless of MLC width. Second, we placed the three targets at

approximately 2 cm from the isocenter. However, the impact of MLC error on the dose distribution depends on the distance between the isocenter and targets. The path length of the beam through the MLC leaf increases as the off-axis distance from the central axis because of the rounded MLC leaf ends[29]. Therefore, the targets that are located far from the isocenter can be strongly affected by the MLC error. Moreover, these effects are greater for the FFF beam than the FF beam [24]. Third, this study was designed to focus only on the MLC error for the DCAT and VMAT techniques, we assumed that the target shape was spherical. The irregular shape or the realistic clinical lesions may be more affected by the MLC error. Thus, future work will focus on noting the target shape. Forth, to clarify the impact of MLC error on the dose distribution, we created the VMAT plan so that the plan quality was equivalent to the DCAT reference plan. Thus, a more complex VMAT plan may be strongly affected by the MLC error. However, we believe that relationship between the plan complexity and MLC error for the VMAT should be investigated in further independent studies. Fifth, we applied the IDL of 80% to the prescribed dose in the reference plan. The lower IDLs (50–70%) will be the dose reduction of normal brain tissue, increasing the internal dose of targets. However, Hofmaier et al. [21] also evaluated the brain SRS treatment plan between the DCAT and VMAT at the 80% IDL prescription. Thus, we believe that this simulation study is sufficient to clarify the characteristics of the MLC errors on the dose distribution even for 80% IDL prescription.

Conclusion

We evaluated the plan robustness of the DCAT and VMAT techniques on the MLC errors in the brain SRS treatment using TPS simulation. The target coverage and the normal brain tissue are comparably affected by the MLC errors for both techniques. Thus, the MLC QC with DCAT tolerance level should be set as equal to that of the VMAT technique. Moreover, we found that the internal dose distribution of the targets generated by the DCAT technique was robust to the MLC errors. Hence,

for the MLC commissioning of DCAT, the DLG parameters should be tuned to match the peripheral dose of the target with the measurement dose.

Conflicts of interest

The authors have no conflicts of interest to declare that are relevant to the content of this article.

Funding

This work was supported by JSPS KAKENHI Grant Number JP23K14842.

Acknowledgment

The authors thank Mr. Akihisa Wakita (EuroMediTech Co., LTD) for his comment on the creation of the python code.

Authors' contributions

Concept and design: H.K.; data analysis: H.K. and T.K.; writing, reviewing and editing: H.K., T.K., M.K., S.T., and T.S. All authors read and approved the final manuscript.

References

1. Gevaert T, Steenbeke F, Pellegri L, et al. Evaluation of a dedicated brain metastases treatment planning optimization for radiosurgery: a new treatment paradigm? Radiat Oncol. 2016; 11: 13, doi: 10.1186/s13014-016-0593-y, indexed in Pubmed: 26831367.
2. Ohira S, Ueda Y, Akino Y, et al. HyperArc VMAT planning for single and multiple brain metastases stereotactic radiosurgery: a new treatment planning approach. Radiat Oncol. 2018; 13(1): 13, doi: 10.1186/s13014-017-0948-z, indexed in Pubmed: 29378610.
3. Raza GH, Capone L, Tini P, et al. Single-isocenter multiple-target stereotactic radiosurgery for multiple brain metastases: dosimetric evaluation of two automated treatment planning systems. Radiat Oncol. 2022; 17(1): 116, doi: 10.1186/s13014-022-02086-3, indexed in Pubmed: 35778741.
4. Chea M, Fezzani K, Jacob J, et al. Dosimetric study between a single isocenter dynamic conformal arc therapy technique and Gamma Knife radiosurgery for multiple brain

metastases treatment: impact of target volume geometrical characteristics. Radiat Oncol. 2021; 16(1): 45, doi: 10.1186/s13014-021-01766-w, indexed in Pubmed: 33639959.

5. Fung NT, Wong WL, Lee MC, et al. Geometric and dosimetric consequences of intra-fractional movement in single isocenter non-coplanar stereotactic radiosurgery. Radiat Oncol. 2023; 18(1): 9, doi: 10.1186/s13014-022-02195-z, indexed in Pubmed: 36631832.
6. Oliver M, Gagne I, Bush K, et al. Clinical significance of multi-leaf collimator positional errors for volumetric modulated arc therapy. Radiother Oncol. 2010; 97(3): 554–560, doi: 10.1016/j.radonc.2010.06.013, indexed in Pubmed: 20817291.
7. Deng J, Huang Y, Wu X, et al. Comparison of dosimetric effects of MLC positional errors on VMAT and IMRT plans for SBRT radiotherapy in non-small cell lung cancer. PLoS One. 2022; 17(12): e0278422, doi: 10.1371/journal.pone.0278422, indexed in Pubmed: 36454884.
8. Ruggieri R, Naccarato S, Mazzola R, et al. Linac-based radiosurgery for multiple brain metastases: Comparison between two mono-isocenter techniques with multiple non-coplanar arcs. Radiother Oncol. 2019; 132: 70–78, doi: 10.1016/j.radonc.2018.11.014, indexed in Pubmed: 30825972.
9. Paddick I. A simple scoring ratio to index the conformity of radiosurgical treatment plans. J Neurosurg. 2000; 93(supplement_3): 219–222, doi: 10.3171/jns.2000.93.supplement_3.0219, indexed in Pubmed: 11143252.
10. Paddick I, Lippitz B. A simple dose gradient measurement tool to complement the conformity index. J Neurosurg. 2006; 105 Suppl: 194–201, doi: 10.3171/sup.2006.105.7.194, indexed in Pubmed: 18503356.
11. Pogson EM, Aruguman S, Hansen CR, et al. Multi-institutional comparison of simulated treatment delivery errors in ssIMRT, manually planned VMAT and autoplan-VMAT plans for nasopharyngeal radiotherapy. Phys Med. 2017; 42: 55–66, doi: 10.1016/j.ejmp.2017.08.008, indexed in Pubmed: 29173921.

12. LoSasso T, Chui CS, Ling CC. Physical and dosimetric aspects of a multileaf collimation system used in the dynamic mode for implementing intensity modulated radiotherapy. Med Phys. 1998; 25(10): 1919–1927, doi: 10.1118/1.598381, indexed in Pubmed: 9800699.
13. Prentou G, Pappas EP, Prentou E, et al. Impact of systematic MLC positional uncertainties on the quality of single-isocenter multi-target VMAT-SRS treatment plans. J Appl Clin Med Phys. 2022; 23(8): e13708, doi: 10.1002/acm2.13708, indexed in Pubmed: 35733367.
14. Minniti G, Clarke E, Lanzetta G, et al. Stereotactic radiosurgery for brain metastases: analysis of outcome and risk of brain radionecrosis. Radiat Oncol. 2011; 6: 48, doi: 10.1186/1748-717X-6-48, indexed in Pubmed: 21575163.
15. Xu Q, Fan J, Grimm J, et al. The dosimetric impact of the prescription isodose line (IDL) on the quality of robotic stereotactic radiosurgery (SRS) plans. Med Phys. 2017; 44(12): 6159–6165, doi: 10.1002/mp.12630, indexed in Pubmed: 29064585.
16. Zhang Q, Zheng D, Lei Y, et al. A new variable for SRS plan quality evaluation based on normal tissue sparing: the effect of prescription isodose levels. Br J Radiol. 2014; 87(1043): 20140362, doi: 10.1259/bjr.20140362, indexed in Pubmed: 25226047.
17. Romano KD, Trifiletti DM, Garda A, et al. Choosing a Prescription Isodose in Stereotactic Radiosurgery for Brain Metastases: Implications for Local Control. World Neurosurg. 2017; 98: 761–767.e1, doi: 10.1016/j.wneu.2016.11.038, indexed in Pubmed: 27867125.
18. Abraham C, Garsa A, Badiyan SN, et al. Internal dose escalation is associated with increased local control for non-small cell lung cancer (NSCLC) brain metastases treated with stereotactic radiosurgery (SRS). Adv Radiat Oncol. 2018; 3(2): 146–153, doi: 10.1016/j.adro.2017.11.003, indexed in Pubmed: 29904739.
19. Khong J, Govindaraj R, Ramm D, et al. Cochlear sparing in LINAC-based radiosurgery for vestibular schwannoma: a dosimetric comparison of dynamic conformal arc, IMRT and VMAT treatment plans. Radiat Oncol. 2023; 18(1): 2, doi: 10.1186/s13014-022-02188-y, indexed in Pubmed: 36600254.

20. Torizuka D, Uto M, Takehana K, et al. Dosimetric comparison among dynamic conformal arc therapy, coplanar and non-coplanar volumetric modulated arc therapy for single brain metastasis. J Radiat Res. 2021 [Epub ahead of print], doi: 10.1093/jrr/rrab092, indexed in Pubmed: 34604907.
21. Hofmaier J, Bodensohn R, Garny S, et al. Single isocenter stereotactic radiosurgery for patients with multiple brain metastases: dosimetric comparison of VMAT and a dedicated DCAT planning tool. Radiat Oncol. 2019; 14(1): 103, doi: 10.1186/s13014-019-1315-z, indexed in Pubmed: 31186023.
22. Kielar K, Mok E, Wang L, et al. SU-E-T-540: Verification of Dosimetric Accuracy on the TrueBeam STx: Rounded Leaf Effect of the High Definition MLC. Med Phys. 2011; 38(6Part19): 3613–3613, doi: 10.1118/1.3612502, indexed in Pubmed: 2303967.
23. Isono M, Akino Y, Mizuno H, et al. Inter-unit variability of multi-leaf collimator parameters for IMRT and VMAT treatment planning: a multi-institutional survey. J Radiat Res. 2020; 61(2): 307–313, doi: 10.1093/jrr/rrz082, indexed in Pubmed: 31927580.
24. Shende R, Patel G. Validation of Dosimetric Leaf Gap (DLG) prior to its implementation in Treatment Planning System (TPS): TrueBeam™ millennium 120 leaf MLC. Rep Pract Oncol Radiother. 2017; 22(6): 485–494, doi: 10.1016/j.rpor.2017.09.001, indexed in Pubmed: 29070960.
25. Kim J, Han JS, Hsia AnT, et al. Relationship between dosimetric leaf gap and dose calculation errors for high definition multi-leaf collimators in radiotherapy. Phys Imaging Radiat Oncol. 2018; 5: 31–36, doi: 10.1016/j.phro.2018.01.003, indexed in Pubmed: 33458366.
26. Vieillevigne L, Khamphan C, Saez J, et al. On the need for tuning the dosimetric leaf gap for stereotactic treatment plans in the Eclipse treatment planning system. J Appl Clin Med Phys. 2019; 20(7): 68–77, doi: 10.1002/acm2.12656, indexed in Pubmed: 31225938.

27. Bruschi A, Esposito M, Pini S, et al. How the detector resolution affects the clinical significance of SBRT pre-treatment quality assurance results. Phys Med. 2018; 49: 129–134, doi: 10.1016/j.ejmp.2017.11.012, indexed in Pubmed: 29203119.

28. Chun M, Kim JI, Oh DH, et al. Effect of dose grid resolution on the results of patient-specific quality assurance for intensity-modulated radiation therapy and volumetric modulated arc therap. Int J Radiat Res. 2020; 3: 521–530, doi: 10.18869/acadpub.ijrr.18.3.521.

29. Kumaraswamy LK, Schmitt JD, Bailey DW, et al. Spatial variation of dosimetric leaf gap and its impact on dose delivery. Med Phys. 2014; 41(11): 111711, doi: 10.1118/1.4897572, indexed in Pubmed: 25370625.

Figure 1. A. The blue contours on the computed tomograpgy (CT) images were 10-mm diameter spheres, which were defined as gros tumor volumes (GTVs). The red contours were defined as planning trget volumes (PTVs), which added a 1-mm margin to the GTVs. Three PTVs were defined as PTV_a, PTV_b and PTV_c, and the distance between iso-center and each PTV was approximately 2 cm; **B.** Dose distribution of the reference plan with the dynamic conformal arc therapy (DCAT) technique

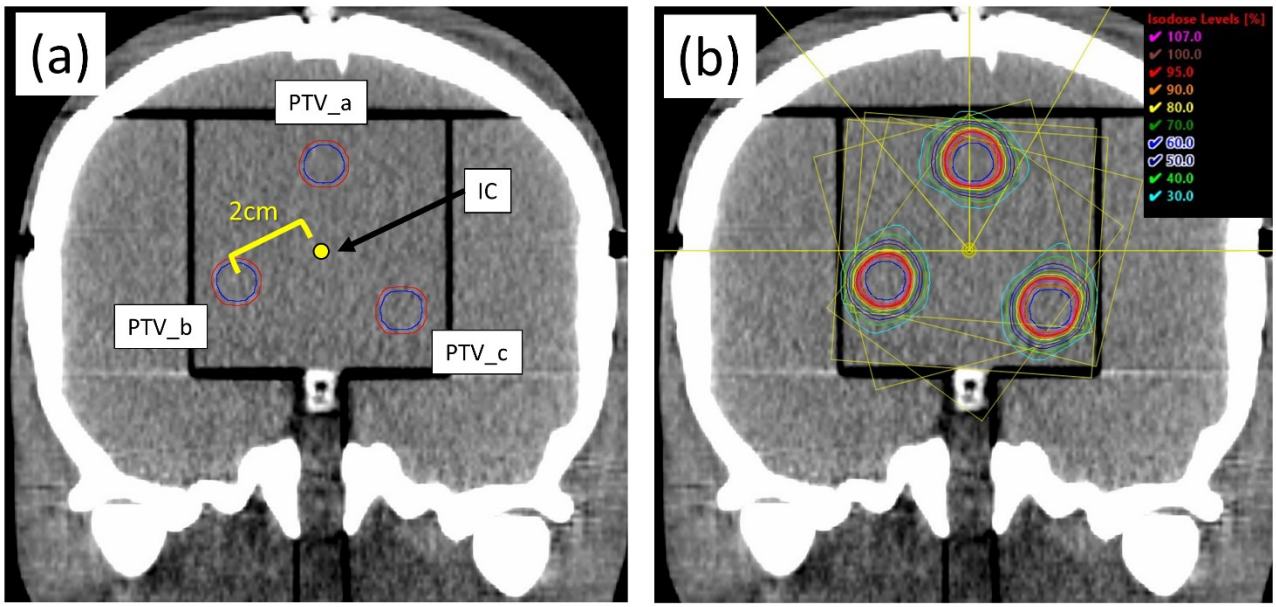

Figure 2. Example of the multi-leaf collimator (MLC) positions with the reference plan and MLC error plans for the dynamic conformal arc therapy (DCAT) and volumetric modulated arc therapy (VMAT) techniques as follows. **A.** Reference plan with the DCAT; **B.** closed 1-mm MLC errors with the DCAT; **C.** reference plan with the VMAT; **D.** closed 1-mm MLC errors with the VMAT

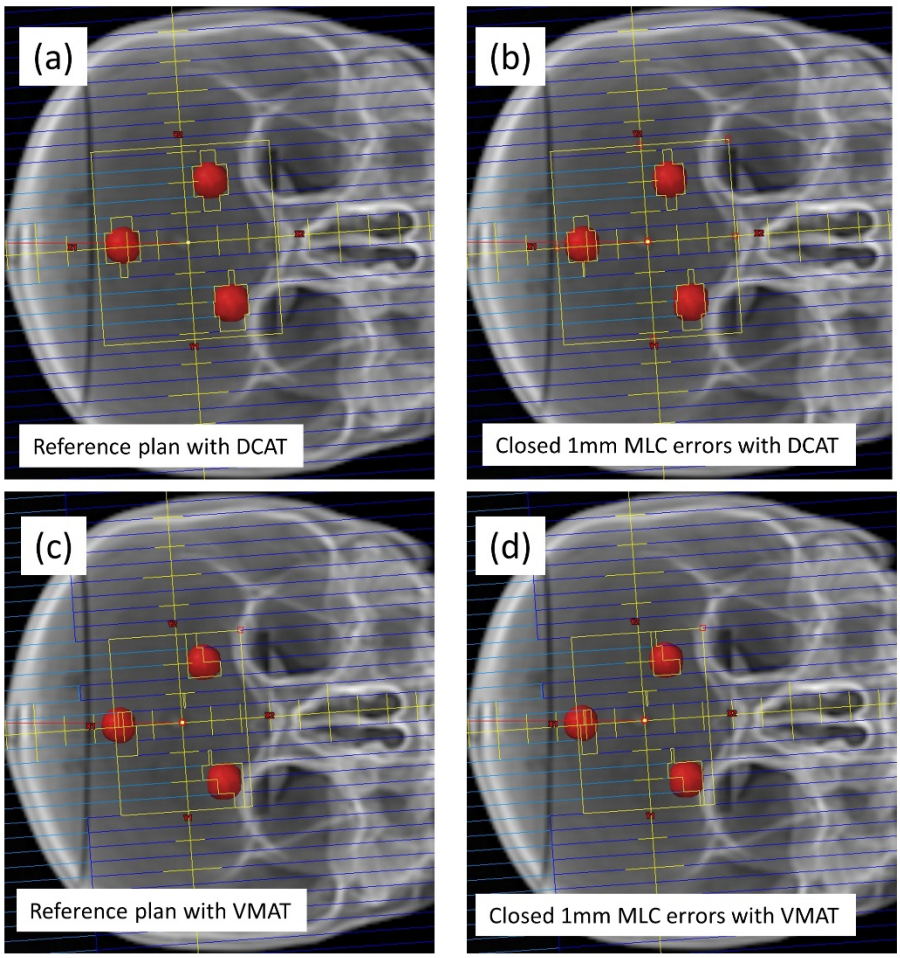

Figure 3. The relationship between the magnitude of multi-leaf collimator (MLC) errors and the mean percentage change in $D_{98\%}$ (Gy) for the planning target volumes (PTVs) from the reference plan with the target diameters of (**A**) 5 mm, (**B**) 10 mm, and (**C**) 15 mm for the dynamic conformal arc therapy (DCAT) and volumetric modulated arc therapy (VMAT) techniques. The error bars indicate the standard deviation for the three PTVs

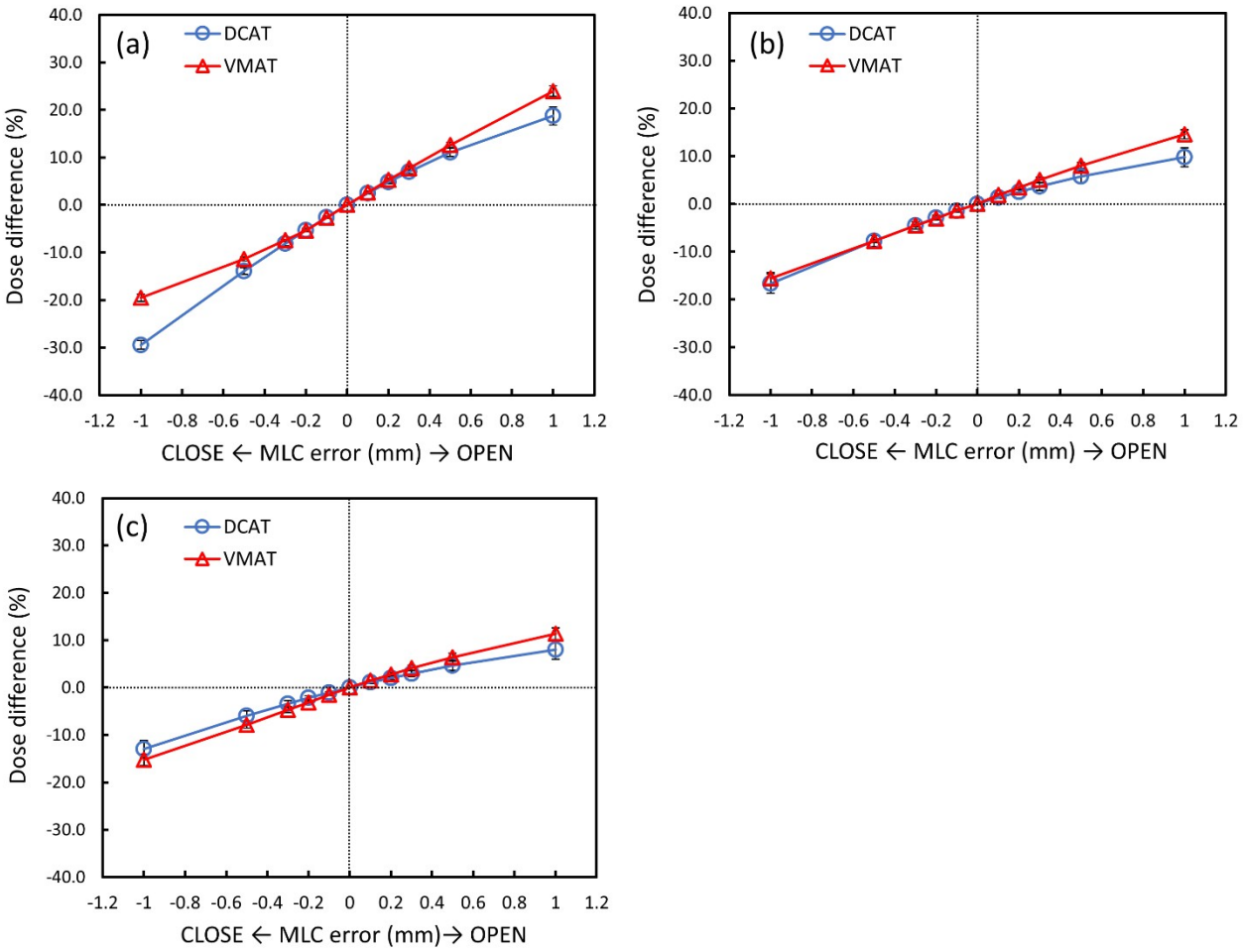

Figure 4. The relationship between the magnitude of multi-leaf collimator (MLC) errors and the mean percentage change in $D_{0.1\%}$ (Gy) for the planning target volumes (PTVs) from the reference plan with the target diameters of (**A**) 5 mm, (**B**) 10 mm, and (**C**) 15 mm for the dynamic conformal arc therapy (DCAT) and volumetric modulated arc therapy (VMAT) techniques. The error bars indicate the standard deviation for the three PTVs

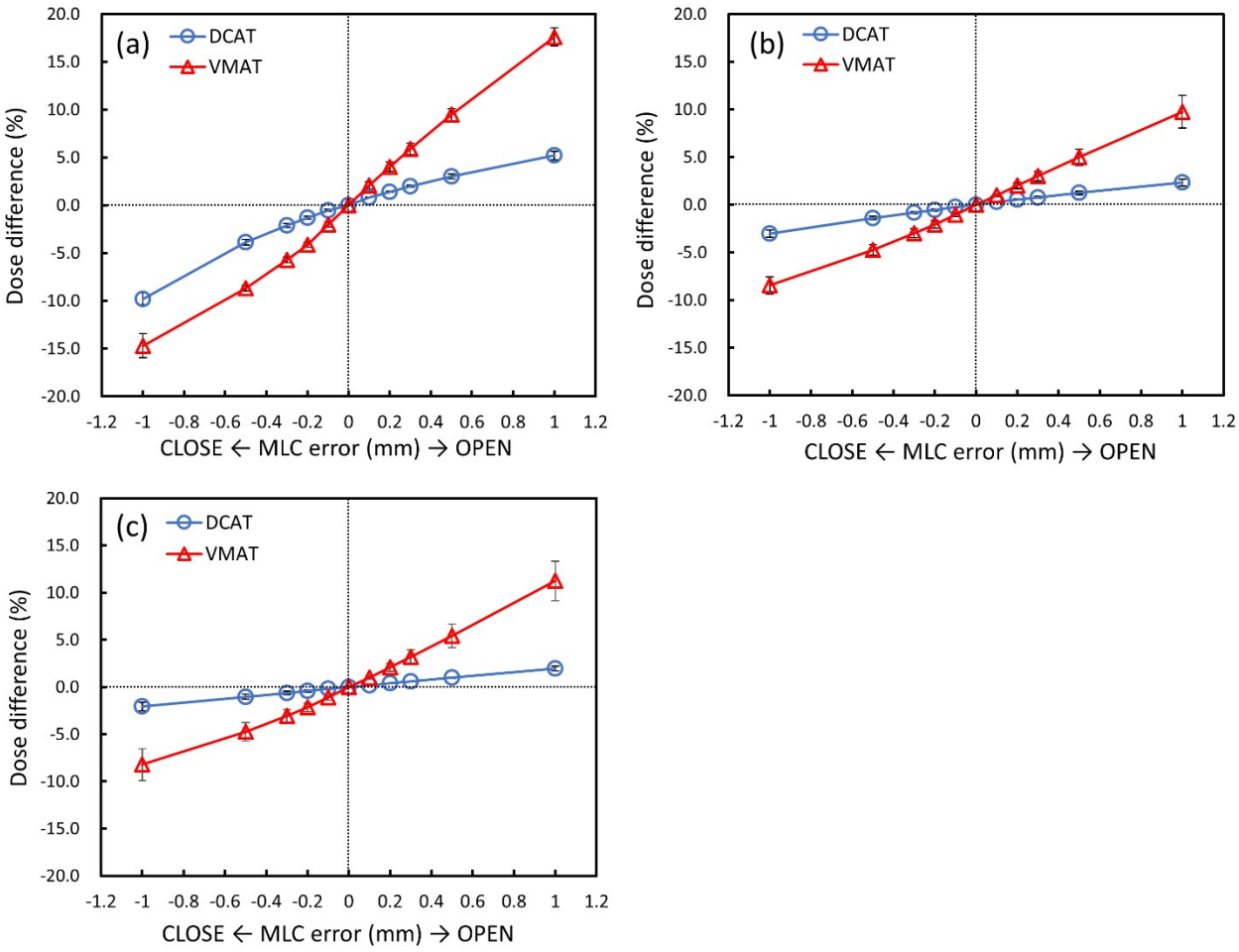

Figure 5. The dose distribution on the computed tomography (CT) images and the dose profiles of planning target volumes (PTVs): PTV_a and PTV_b for dynamic conformal arc therapy (DCAT) (**A**, **B**) and volumetric modulated arc therapy (VMAT) (**C**, **D**) techniques for the target diameter of 10 mm. The dose profile positions were indicated by the yellow line on the CT images. The red and cyan profiles represent the reference plan and the closed 1.0 mm multi-leaf collimator (MLC) error plan, respectively. Internal dose of targets generated by the VMAT was more strongly affected by the MLC errors than that of the DCAT technique (indicated by black arrows)

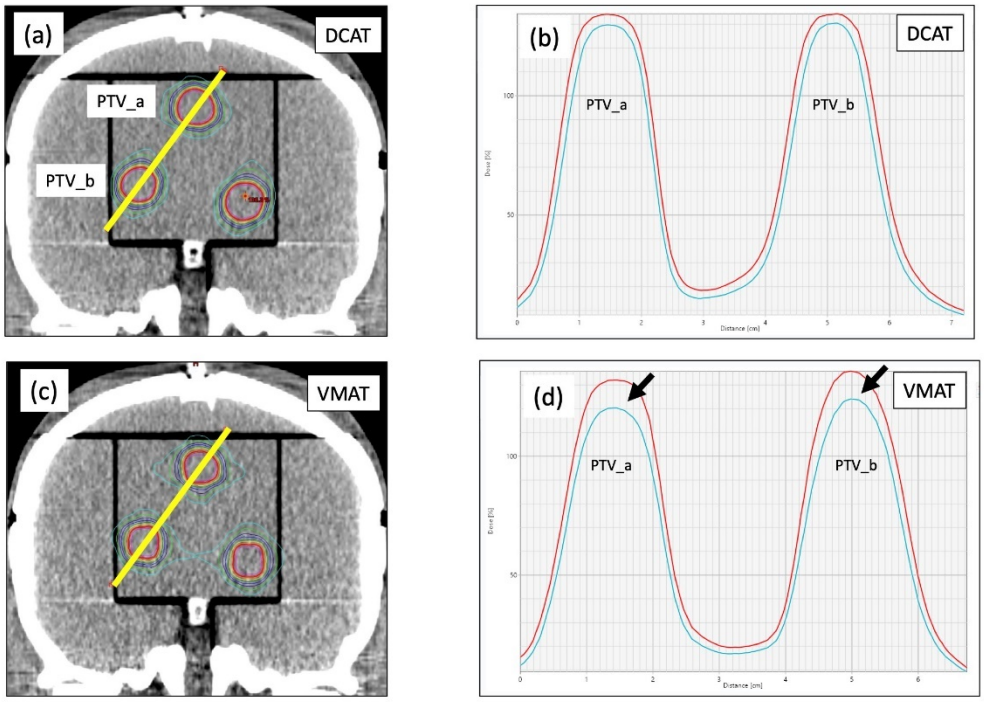

Figure 6. The relationship between the magnitude of multileaf collimator (MLC) errors and the mean percentage change in V_{12Gy} (cc) for the normal brain tissue from the reference plan with the target diameters of 5 mm (**A**), 10 mm (**B**) and 15 mm (C) for the dynamic conformal arc therapy (DCAT) and volumetric modulated arc therapy (VMAT) techniques

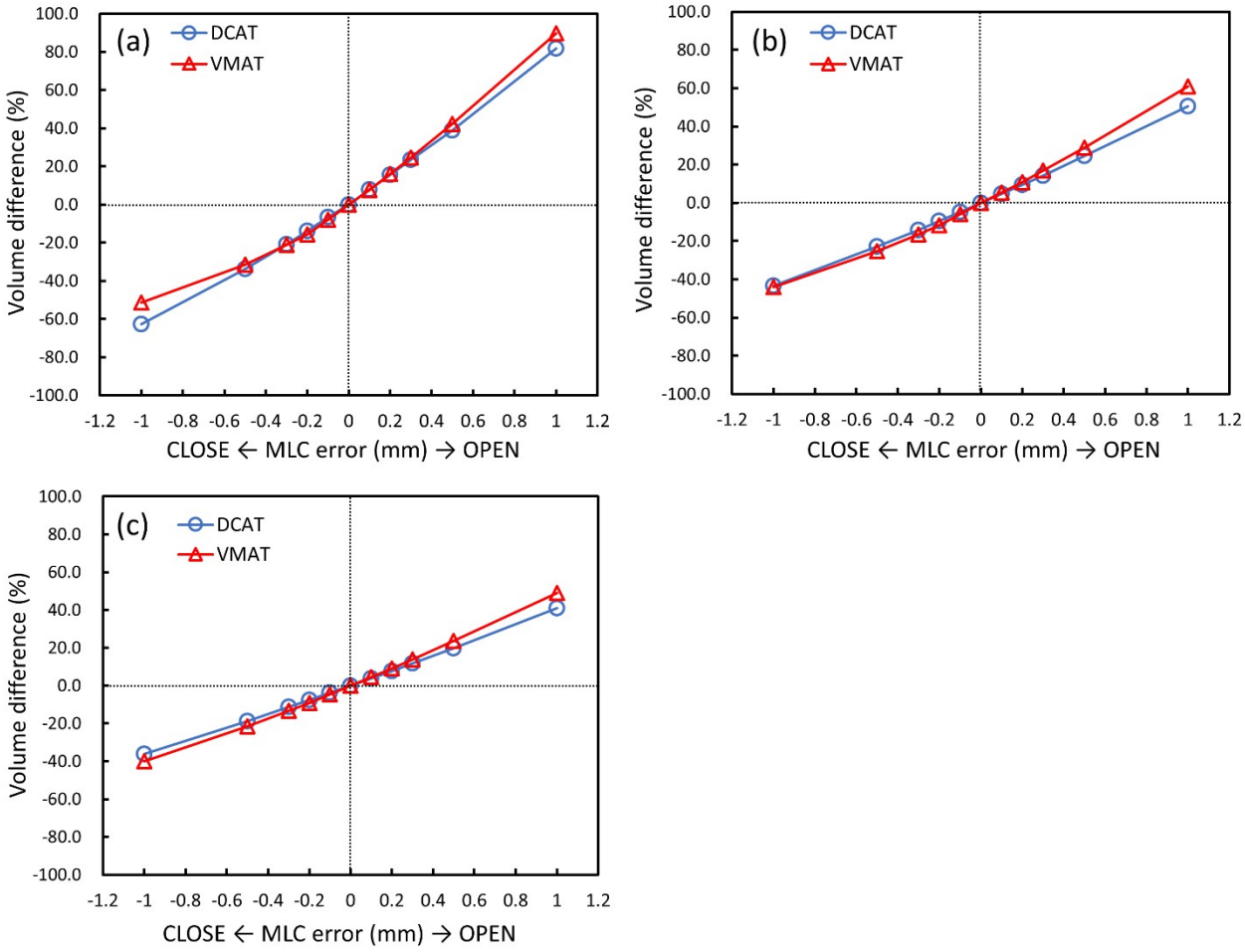

Figure 7. The relationship between the magnitude of multileaf collimator (MLC) errors and the change in conformity index (CI) with target diameter of 5 mm (**A**), 10 mm (**B**), and 15 mm (**C**), and gradient index (GI) with target diameter of 5 mm (**D**), 10 mm (E) and 15 mm (F), from reference plan for the dynamic conformal arc therapy (DCAT) and volumetric modulated arc therapy (VMAT) techniques

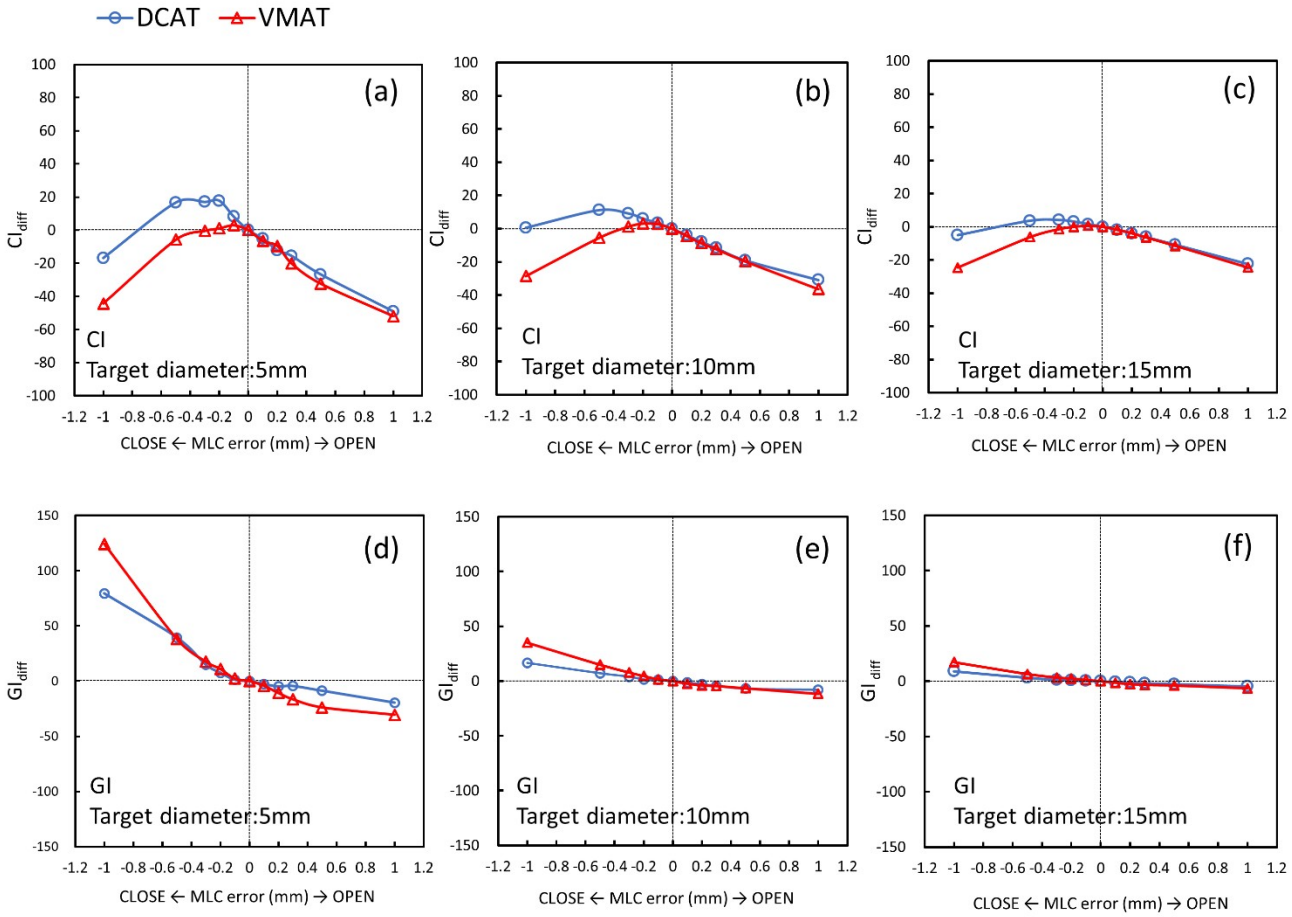

Figure 8. The gamma pass rate (GPR) between the reference plan and each multi-leaf collimator (MLC) error plan for the dynamic conformal arc therapy (DCAT) and volumetric modulated arc therapy (VMAT) techniques as follows. Target diameter of 5 mm (**A**), 10 mm (**B**), and 15 mm (C) with dose threshold 10% and target diameter of 5 mm (**D**), 10 mm (**E**) and 15 mm (F) with dose threshold 40%. The GPR criteria was applied the local dose normalization of 2%/1 mm.

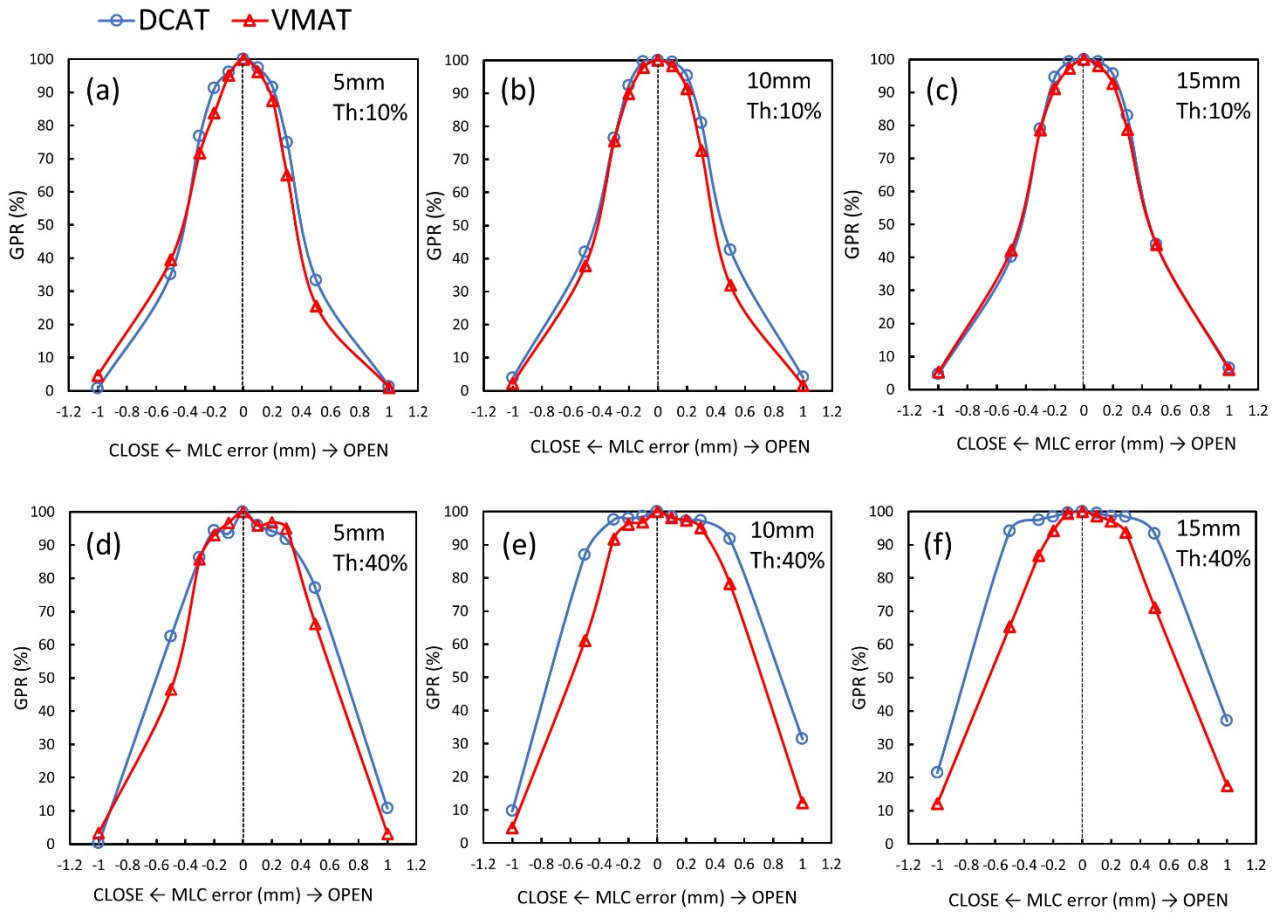

Table 1. Dose-volume histogram (DVH) and plan parameters of the reference plan with the dynamic conformal arc therapy (DCAT) and volumetric modulated arc therapy (VMAT) techniques

Target diameter [mm]	**Technique**	**Number of arcs (non-coplanar)**	**MU**	**Reference plan parameters**				
				PTVs		**Brain-PTVs**	**CI**	**GI**
				$D_{98\%}$ [Gy]	**$D_{0.1\%}$ [Gy]**	**V_{12Gy} [cc]**		
5	DCAT	5(3)	6822	21.8 ± 0.01	28.2 ± 0.27	2.3	0.58	4.66
	VMAT		9594	20.0 ± 0.11	28.0 ± 0.36	2.6	0.52	6.45
10	DCAT	5(3)	5951	21.0 ±	27.0 ±	7.4	0.72	3.7

				0.24	0.18			0
	VMAT		6655	19.9 ± 0.48	27.1 ± 0.25	7.5	0.79	4.48
15	DCAT	6(4)	5998	20.6 ± 0.09	26.3 ± 0.32	14.9	0.82	3.31
	VMAT		7224	20.1 ± 0.08	26.2 ± 0.03	15.0	0.87	3.76

The $D_{98\%}$ (Gy) and $D_{0.1\%}$ (Gy) values were mean ± standard deviations of theplanning target columes (PTVs). Numbers in parentheses indicate the non-coplanar arcs. MU — Monitor unit; CI — conformity index; GI — gradient index

Table 2. The slope value of the linear regression analysis between the magnitude of multi-leaf collimator (MLC) errors and change in the dose-volume histogram (DVH) parameters in each target diameter and technique. The slope value indicates the dose percentage change per millimeter of the MLC errors for the dynamic conformal arc therapy (DCAT) and volumetric modulated arc therapy (VMAT) techniques

DVH parameters	**Target diameters [mm]**	**Techniques**			
		DCAT		**VMAT**	
		slope	**R^2**	**slope**	**R^2**
$D_{98\%}$ [Gy]	5	24.4	0.964	22.5	0.989
	10	13.3	0.950	15.3	0.998
	15	10.5	0.998	13.6	0.982
$D_{0.1\%}$ [Gy]	5	7.3	0.930	16.9	0.989
	10	2.7	0.982	9.3	0.995
	15	2.0	0.999	9.9	0.982
$V_{12\ Gy}$ [cc]	5	72.5	0.986	71.7	0.946
	10	47.1	0.996	53.2	0.981

	15	38.5	0.997	44.7	0.993